Mon. Not. R. Astron. Soc. **302,** 677–683 (1999)

Supersonic gas motion in giant extragalactic H II regions

Jorge Melnick,[1] Guillermo Tenorio-Tagle[2,3,4] and Roberto Terlevich[5]

[1] *European Southern Observatory, Casilla 19001, Santiago 19, Chile*
[2] *INAOE, Apartado Postal 51, 72000, Puebla, Mexico*
[3] *Institute of Astronomy, Madingley Road, Cambridge CB3 0HA*
[4] *Instituto de Astrofisica de Canarias, La Laguna, Tenerife, Spain*
[5] *Royal Greenwich Observatory, Madingley Road, Cambridge CB3 0HA*

Accepted 1998 September 8. Received 1998 July 14; in original form 1998 February 27

ABSTRACT

We present high signal-to-noise ratio, long-slit spectra of the central region of the 30 Doradus nebula taken with unprecedented spatial (∼0.1 pc) and spectral (∼3 km s^{-1}) resolution. We use these observations to investigate the dominant line-broadening mechanisms for the global nebula. We find no evidence for significant gravitational broadening of the lines. Thus, broadening appears to be dominated by stellar winds and thermal motions. However, we identify a new broad component to the lines that explains the integrated profile wings identified in previous observations. The broad component appears at all positions observed, and is possibly related to the disruption through photo-evaporation of high-density condensations within the nebula.

Key words: H II regions – ISM: individual: 30 Doradus – ISM: kinematics and dynamics.

1 INTRODUCTION

1.1 Background

More than their large sizes, the key defining property of giant H II regions (GH IIRs), as a distinct class of objects, is the supersonic velocity widths of their integrated emission-line profiles (Smith & Weedman 1972; Melnick 1977; Melnick et al. 1987, and references therein). Since supersonic gas motions will rapidly decay due to the formation of strong radiative shocks, the detection of Mach numbers greater than 1 in the nebular gas poses an astrophysically challenging problem.

Melnick (1977) suggested that the ionized gas is made of dense clumps moving in an empty or very tenuous medium, so that the integrated profiles reflect the velocity dispersion of discrete clouds rather than hydrodynamical turbulence. In this model, the relevant time-scale for radiative decay of the kinetic energy is the crossing-time of the H II regions, which turns out to be comparable to the ages of the ionizing clusters. This idea was refined by Terlevich & Melnick (1981), who showed that the sizes (R) and luminosities (L) of giant H II regions correlate with velocity dispersion (σ) as $R \propto \sigma^2$, and $L \propto \sigma^4$ ($\sigma = 0.425$ FWHM). Terlevich & Melnick also showed that these two correlations extend to a similar but more luminous class of objects called H II galaxies. The fact that these correlations are similar to the relations exhibited by virialized self-gravitating stellar systems such as globular clusters, spiral bulges, and elliptical galaxies led Terlevich & Melnick to propose that GH IIRs and H II galaxies themselves are virialized systems, and therefore that the velocity dispersion of the gas is a direct measure of their total mass. Although Gallagher & Hunter (1983) failed to confirm the relations in a particular sample of extragalactic nebulae,[1] the Terlevich & Melnick relations have been subsequently confirmed by Hippelein (1986) and Roy, Arsenault & Joncas (1986), and definitively established and calibrated by Melnick et al. (1987) and Melnick, Terlevich & Moles (1988), albeit with slopes slightly different to those found by earlier papers. It is interesting to note in this context that the analysis of more complete data sets for elliptical galaxies also yields slopes somewhat different from the scaling laws resulting from the simplest application of the virial theorem (see Busarello et al. 1997 for a recent review).

Tenorio-Tagle, Mũnoz-Tuñón & Cox (1993) proposed a model called the *Cometary Stirring Model* (CSM) to explain the origin and persistence of the supersonic gas motions. In the CSM, kinetic energy is continuously injected to the interstellar medium by the bow shocks and wakes caused by low-mass stars undergoing winds while moving in the gravitational potential of the ionizing clusters. The gas thus stirred is subsequently ionized by massive stars which form at a later stage in the collapse. The CSM predicts that the nebular gas profiles in the densest regions of GH IIRs should be smooth and well approximated by Gaussians of widths $\sigma_{\rm vir} = \sqrt{GM/R}$.[2] Extremely high spatial resolution observations would be required to resolve individual bow shocks and wakes.

Thus, in both gravity-driven models, the global line profile is made of individual 'clouds' (filaments) of gas moving at supersonic velocities. The main difference is that the CSM scenario is able to support and maintain the supersonic motions owing to the energetics of a large number of low-mass stars, while in the pure

[1] This result is now understood as due to the fact that their sample was dominated by H II regions with subsonic linewidths.

[2] There are two other parameters for the linewidth usually quoted in the literature: FWHM $= 2.355\sigma$ and $\beta = \sqrt{2}\sigma$.

gravitational model collisions and dissipation in shocks will rapidly deplete the number of clouds.

An entirely different broadening mechanism was investigated by Dyson (1979), who proposed that the observed line profiles reflect the combination of several unresolved stellar wind-driven expanding shells and filaments. In order to match the observed line profiles, Dyson's model required the expansion motions to be driven by the combined effects of groups of tens to hundreds of stars, all having essentially the same ages. In this model, the core of the global line profiles is produced by an ionized but dynamically unperturbed medium with a thermal velocity. There is indeed ample observational evidence for the presence of expanding shells in nearby nebulae (Meaburn 1981, 1984; Rosa & Solf 1984), a fact that has led several authors to adhere to stellar wind-driven shocks as the dominant line-broadening mechanism in GH IIRs (Rosa & Solf 1984; Chu & Kennicutt 1994, and references therein). This scenario, however, has been recently analysed in detail by Tenorio-Tagle, Muñoz-Tuñón & Cid-Fernandez (1996), who modelled the integrated emission-line profiles of collections of unresolved expanding shells for a wide range of input parameters. They concluded that, unless the age distribution of the ionizing stars is unusually strongly peaked, the resulting line profiles are always flat-topped, contrary to what is observed. This conclusion was, in fact, anticipated by Dyson (1979), who concluded that star formation in GH IIRs had to be coeval and not sequential. The detailed numerical models, however, show that the age spread required to fit the observations is significantly shorter than the time-scale for gravitational collapse of the protostellar cloud, a result that rules out expanding shells as the sole line-broadening mechanism. Thus, while shells can account for the wings of the integrated profiles, something else is needed to explain the supersonic line cores.

The advent of large panoramic detectors has recently allowed very detailed investigations of the kinematics of GH IIRs in Local Group galaxies. Meaburn (1984, and references therein) used a dedicated spectrograph to study the gas kinematics of 30 Doradus, the largest H II regions in the LMC, along three parallel lines each 238-pc long. He found that the kinematics were dominated by expanding sheets and shells driven by stellar winds of massive stars within the nebula. Meaburn's observations were expanded by Chu & Kennicutt (1994, hereafter C&K), who used the long-slit mode of the CTIO 4-m echelle spectrograph to map the gas motions in 30 Doradus along many lines across the phase of the nebula. They concluded that the overall line profile broadening (i.e., the profile that would be observed through a large aperture encompassing the entire nebula) is dominated by expanding shells and thermal motions, and found no evidence for an unresolved Gaussian component of supersonic width as predicted by the CSM of Tenorio-Tagle et al. (1993). This view contrasts with that of Yang et al. (1996) and Muñoz-Tuñón et al. (1996) who, using Fabry–Pérot observations at a resolution of a few parsecs, obtained and processed independently with TAURUS I at the 2.5-m INT and TAURUS II at the 4.2-m WHT at La Palma, showed that the line profiles in the brightest parts of NGC 604, the largest H II region in M33, are well fitted by *single* Gaussians of (supersonic) widths consistent with $\sqrt{GM/R}$, while the profiles of the outer, fainter, regions appear to be dominated by a few, well-resolved, expanding shells. Both investigations concluded that virial motions and expanding shells contribute roughly equally to the velocity width of the integrated profile of NGC 604. Muñoz-Tuñón (1994) has also used the supersonic single Gaussians to actually define the 'kinematic core' as the region producing such lines. The physical reality of these cores is confirmed by the fact that the scatter in the relation between size and line-width for GH IIRs in M101, NGC4214 and NGC4449 is significantly reduced when the values for the kinematic cores are used instead of the global ones.

Muñoz-Tuñón et al. (1996) also presented data for the second largest H II region in M33 (NGC 588). A very interesting result is that, while the profiles have supersonic widths everywhere in NGC 604, in NGC 588 the situation is more like that in 30 Dor, and subsonic widths are observed over a substantial fraction of the nebula. Muñoz-Tuñón et al. have suggested that this may be an evolutionary effect whereby the dominant line-broadening mechanism in young H II regions is gravity, while wind-driven shells dominate in older nebulae. However, as pointed out recently by Tenorio-Tagle et al. (1997), the situation is more complicated than this simple picture, since the nebular gas kinematics are affected not only by the current generation of massive stars, but also by the previous one(s).

While Muñoz-Tuñón et al. (1996) developed a method to analyse the pixel-to-pixel variations in the line-profile widths over the nebulae, Medina-Tanco et al. (1997) analysed the pixel-to-pixel variations in radial velocity using the same TAURUS II data set. From a study of the (radial velocity) autocorrelation and structure functions they concluded that the kinetic energy spectrum is consistent with a double cascade of subsonic turbulence in two dimensions, probably forced by mass-loss from the most massive stars. While potentially interesting, this result suffers from serious observational biases, since it is based on single-Gaussian fits to the TAURUS II profiles. This approach is not valid in the regions where the profiles are multiple and dominated by expanding shells, and it does not take into account the dominant broadening mode (the supersonic linewidths) in the brightest central regions, thus leaving supersonic motions unexplained.

To summarize, recent observations point to the following as the dominant line-profile broadening mechanisms in GH IIRs.

(i) Thermal broadening. This is a Gaussian effect of characteristic width $\sigma_{\rm th} = \sqrt{kT_{\rm e}/m_{\rm H}}$ ($\simeq 9.1\,{\rm km\,s^{-1}}$ for hydrogen gas at an electronic temperature $T_{\rm e} = 10^4$ K).

(ii) Virial broadening. This is the effect of the total (stars, gas and dust) gravitational field of the region, and is characterized by a Gaussian of width $\sigma_{\rm vir} = \sqrt{GM_{\rm T}/R_{\rm G}}$, where $M_{\rm T}$ is the total mass, and $R_{\rm G}$ is a measure of the size of the mass distribution. Note that, even in the nearest GH IIRs, it is rather difficult to determine either $M_{\rm T}$ or $R_{\rm G}$ observationally.

(iii) Expanding shells and filaments. This mechanism contributes mostly to the formation of the integrated profile wings. These wings are well approximated by Gaussians of typical width $\sigma_{\rm shells}$ (with the caveat that shell profiles are flat-topped, and therefore their cores are not well represented by Gaussian functions).

(iv) Radial velocity dispersion. The radial velocity dispersion of the gas must be included in the total profile decomposition. This is a Gaussian effect of characteristic width $\sigma_{\rm rad}$. At least to first approximation, this width also includes turbulent energy cascades such as that advocated by Medina-Tanco et al. (1997).

The total linewidth (corrected for instrumental effects) is therefore given by $\sigma_{\rm observed} = \sqrt{\sigma^2_{\rm vir} + \sigma^2_{\rm th} + \sigma^2_{\rm shells} + \sigma^2_{\rm rad}}$.

The contribution of other mechanisms, such as large scale shear, rotation, or Champagne flows from neutral and molecular clouds embedded in the nebulae, appears to be comparatively small and will not be considered here, although they are admittedly not well

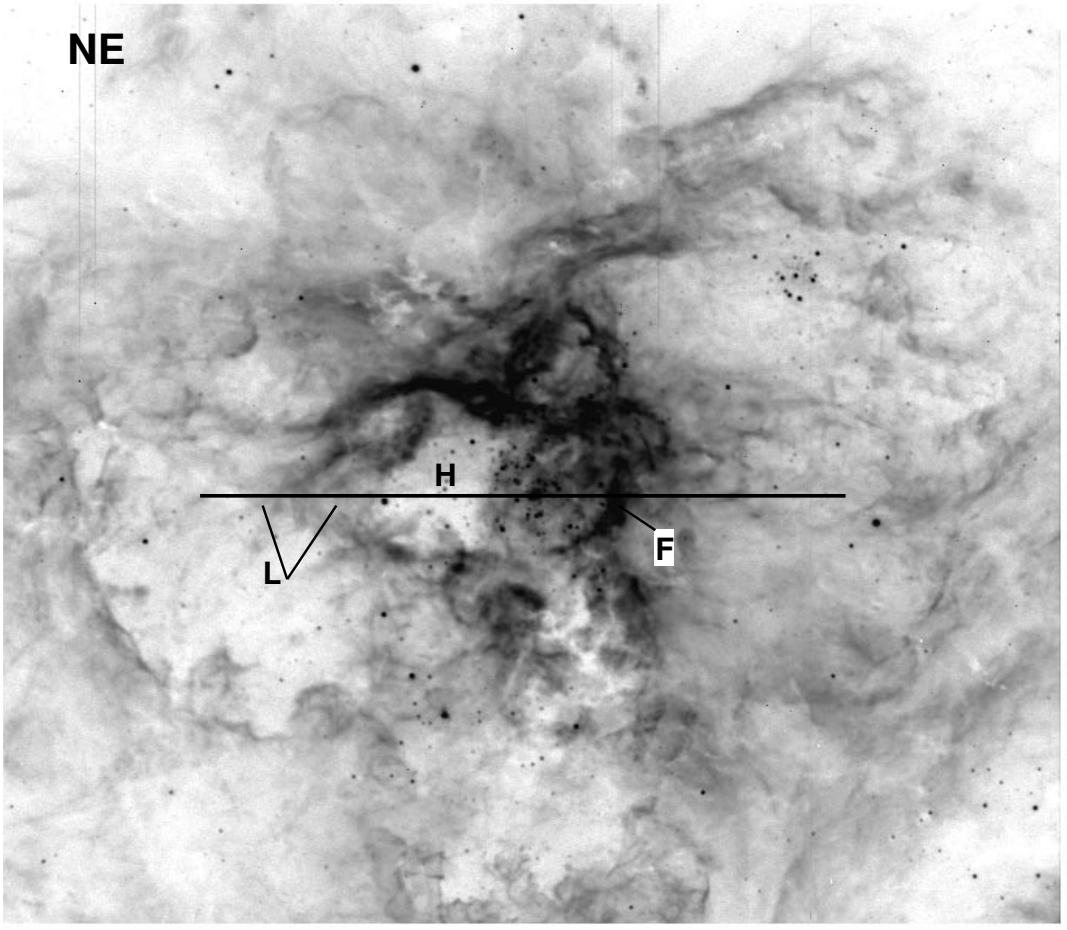

Figure 1. Hα image of the 30 Doradus nebula taken with EMMI at the NTT. The position and the length of the slit (330 arcsec) used in the echelle observations are shown. Several characteristic regions of the spectrum are indicated.

constrained by observations (Dyson 1979; Roy et al. 1986; C&K; Medina-Tanco et al. 1997).

1.2 The virial broadening test

A simple test for the existence and relative importance of virial broadening can be obtained from observations with very high spatial resolution. Any narrow (pencil) beam through a nebula should yield line profiles made of a number of discrete shell components superimposed on a smooth, unresolved, Gaussian component of width $\sqrt{\sigma_{\rm vir}^2 + \sigma_{\rm th}^2}$. In fact, the models and the observations of NGC 604 discussed above indicate that $\sigma_{\rm vir}$ is only felt by the gas in the kinematic cores of the H II regions, while the profiles in the outer parts appear to be dominated by large-scale expansion motions. If this is generic to GH IIRs, then smooth supersonic components should appear only in pencil beams through the brightest central parts of the H II regions.

We will refer to this simple experiment as the *virial broadening test*. Clearly, the higher the spatial resolution, the cleaner the results of this test will be. In this paper we present new high spatial and velocity resolution observations of the nearest GH IIR 30 Doradus. Our observations are a refinement of the work by C&K specifically aimed at applying the test with a resolution of ~ 0.1 pc The interested reader is kindly referred to the article by C&K for a comprehensive view of the gas motions in 30 Dor, at substantially lower spatial and spectral resolutions.

2 OBSERVATIONS

High-resolution observations of 30 Doradus were obtained 1995 October 7 with the echelle long-slit mode of EMMI at the 3.5-m NTT telescope on La Silla. A 73-Å wide interference filter centred at 6559.1 Å was used for order separation. The spectrum was recorded on a Tektronix 2048×2048 CCD with 24-μm pixels corresponding to 0.27 arcsec on the sky. The slit was 0.6 arcsec wide and 330 arcsec long. The dispersion was 0.067 Å pixel^{-1} and the instrumental resolution measured on a Th-Ar calibration spectrum is 0.15 Å (FWHM; 2.2 pixel) or, correspondingly, $\sigma_{\rm instr} = 3\,{\rm km\,s^{-1}}$.

The instrumental profile is very well approximated by a single Gaussian function. The wings of the instrumental profile, which are of relevance to the present discussion, are over-represented by the Gaussian fit, which gives slightly more power to the wings than the actual profile at the < 1 per cent level.

Two 1800-s exposures were obtained under photometric weather and excellent seeing conditions (< 0.6 arcsec FWHM). At the distance of the LMC (50 kpc) the seeing disc corresponds to 0.13 pc, while each pixel covers about half that size. Our sampling is therefore significantly better than any previous spectroscopic observations (C&K; Hunter et al. 1995), and also has higher S/N ratio.

Fig. 1 shows a 1-min Hα image of 30 Doradus, taken with the same instrument (EMMI) through the same Hα filter used as

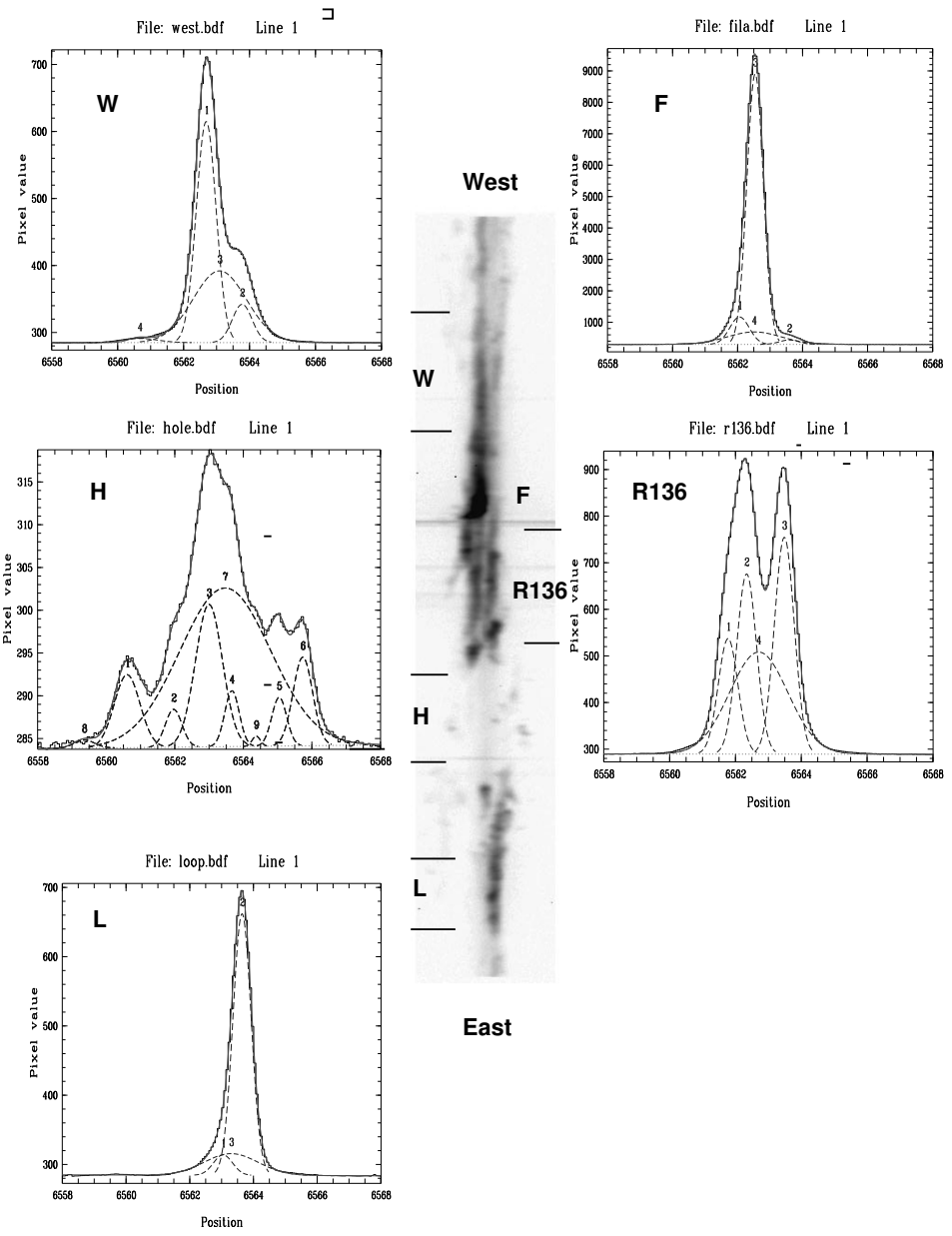

Figure 2. Long-slit echelle spectrum of 30 Doradus taken with EMMI at the NTT. The slit is oriented east–west, as indicated in Fig. 1. A number of characteristic regions of the spectrum are labelled with references to the direct image. Tracings of the sum of all spectral rows within these subregions (indicated by horizontal lines above and below the label for each region) are also shown together with multiple Gaussian fits. Notice the large range in peak intensities of more than a factor of 30 from F to H.

order separator. The image covers an area of 8×8 arcmin^2 at a pixel resolution of 0.27 arcsec pixel^{-1}. The seeing disc measured on this image is about 1.5 arcsec FWHM. The position of the slit (indicated in the image) was selected to pass as close as possible to the core of the ionizing cluster (R136) without including it in order to avoid excessive contamination by starlight. The exact position was chosen to include the brightest parts of filament 'F' and emptiest region of the breakout region 'H'.

3 RESULTS

3.1 Spectral morphology

The central part (Hα) of the wavelength-calibrated median of the two exposures, rebinned to a wavelength scale in the rest frame of the nebula, is reproduced in Fig. 2. Multicomponent Gaussian fits to several representative sections of the spectrum as discussed below are also shown.

Although none of the morphological features shown in our spectrum are really new, they are seen here at substantially higher spatial and spectral resolution than previous work, and therefore give us new insights into the physical processes at work. We have labelled three relevant sections of the spectrum on the Hα image shown in Fig. 1. From east to west, the relevant features are as follows.

(i) The 'loop'. This feature is labelled L in Fig. 1, and corresponds to the edge of one of the most prominent loops in the Tarantula. As shown in the tracing, the integrated profile of this region is dominated by a single component, which is redshifted with respect to the nebula as a whole.

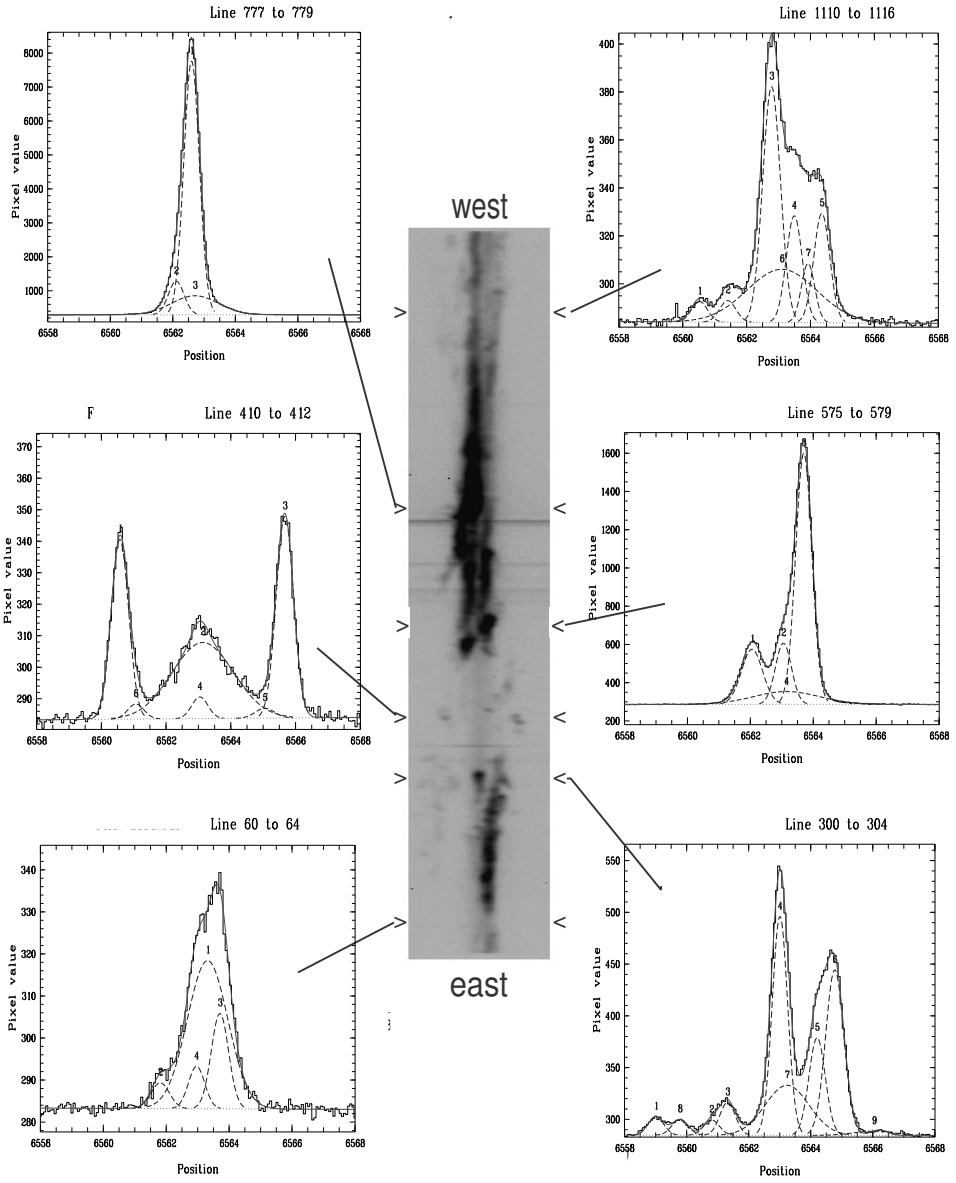

Figure 3. Representative line profiles at several positions along the slit. Each tracing corresponds to the average of 2–7 lines, and thus preserves the full spatial resolution of the original 2D spectrum. Multiple Gaussian fits are plotted with each cut. Notice that the broad component is present in all tracings.

(ii) The 'hole'. This feature is labelled H in the Hα image. The spectrum in this feature is dominated by a faint, broad ($\sigma \sim 1$ Å) component centred at the radial velocity of the nebula. A number of blobs of gas moving at large velocities are also revealed by the spectrum in this region. A close inspection of the 'hole' shows that the slit passes exactly over a 'white' filament. This may be a region of extremely weak emission, or of extremely high extinction since molecular clouds are present in the central region of the Tarantula (Poglitsch et al. 1995). There are numerous blobs of gas seen in the region of the hole, some moving with velocities of more than $100\,\mathrm{km\,s^{-1}}$ with respect to the nebula. This suggests that this and similar holes seen in other regions of the nebula (e.g. C&K) are regions where expanding wind-driven shells undergo 'breakout' (Tenorio-Tagle et al. 1997, and references therein).

(iii) The 'core'. This region is not labelled in the image. It corresponds to the region near the core of the cluster (R136), which is clearly visible at the centre of the image. The spectrum here is dominated by two strong components separated by 1.2 Å, or $55\,\mathrm{km\,s^{-1}}$ in velocity. The width of both components is close to $\sigma_{\mathrm{observed}} = 0.3$ Å, or about $13.7\,\mathrm{km\,s^{-1}}$.

(iv) The 'filament'. This feature labelled F in the image corresponds to the bright filament east of the core, and is the brightest part of our spectrum. This filament is one of the most characteristic structures of the Tarantula nebula, which, in fact, contribute to giving it this name. The spectral line is dominated by a strong component centred at $-11\,\mathrm{km\,s^{-1}}$, and a second one, about 3 times weaker, centred at $-34.3\,\mathrm{km\,s^{-1}}$. Both components, however, are stronger than any other feature in the spectrum.

(v) The western side. Immediately to the west of the bright filament the image shows a complex filamentary structure, and the spectrum has strong lines with multiple components. Beyond this region the spectrum shows fairly strong emission, with two components dominating.

3.2 Resolved line profiles

1D tracings of the spectrum at six representative velocity cuts along the slit, preserving the spatial resolution (2–7 pixels) are presented in Fig. 3. Multiple Gaussian components have been fitted to these 1D profiles using MIDAS. While these fits are by no means unique, they are useful for characterizing the different velocity systems that make up the profiles. The first impression one gets from these cuts is that, even at the brightest positions in the nebula, more than one Gaussian component is needed to fit the data. A closer inspection of the fits shows that, in order to fit the wings of the lines, a broad component ($\sigma_{\rm broad} \sim 1$ Å) is required for all cuts. In fact, in the 'Hole' region the broad component dominates the emission, and is in fact clearly visible in the 2D spectrum. We have carefully checked that this component is not instrumental by analysing the lines from a reference Th-Ar spectrum which are very well fitted by a single Gaussian. The fact that the broad component appears in regions where there are hardly any other components at all provides further evidence for its reality. We will return to this component in the next section.

All the other components of all fits have subsonic velocity widths of order 0.3 Å, and even at the brightest spot (lines 777–779) there is no evidence for any unresolved supersonic component besides the very broad component described above.

The spectrum can thus be characterized by shells, pieces of shells, clumps, and filaments with internal turbulent motions typically $< 6\,{\rm km\,s^{-1}}$ moving in some cases at very large velocities with respect to each other (e.g., lines 410–412 show two, albeit faint components, flying apart at about $250\,{\rm km\,s^{-1}}$).

4 THE VIRIAL BROADENING TEST

The description of the observational results presented above already contains the answer to the test: there are no regions in the spectrum which present unresolved components of supersonic velocity widths, $\sigma_{\rm turb} \sim 20\,{\rm km\,s^{-1}}$. Even in the brightest regions close to the cluster core, any line of sight intercepts at most a few discrete components. Therefore, most of the emission originates in clumps, shells and filaments of sizes larger than our spatial resolution (i.e., larger than about 0.1 pc). In fact, the 2D spectrum presented in Fig. 2 shows the lines to be clumpy on that scale in the spatial direction as well.

An unexpected result is the presence of the broad component necessary to reproduce the wings of the profiles at all positions along the slit. Although this component changes somewhat in radial velocity and width along the slit, these variations are consistent, to the extent that the number of Gaussian components used to fit each profile is arbitrary, with constant width and radial velocity at all positions. Thus the broad component appears to be at rest relative to the centroid of the nebula, with a dispersion, after correction for instrumental and thermal broadening, of $\sigma_{\rm broad} = 45\,{\rm km\,s^{-1}}$. We have made many experiments to try to fit the profiles by replacing the broad component with several narrower ones, without success. We are confident, therefore, that the broad component is real and not due to instrumental or numerical effects, although we cannot be absolutely sure. In working with this component, however, we were reminded of the integrated profile obtained by C&K by adding all their echelle spectra. According to these authors, the integrated profile shows broad, non-Gaussian wings, which they attributed to the rapidly expanding shells and networks in the outer regions of the nebula. Rob Kennicutt has kindly sent us the data to try a multi-component fit. This is shown in Fig. 4 which shows that the integrated profile can be very well fitted by two Gaussians at the same radial velocity, with widths, corrected for thermal and instrumental broadening, of $\sigma_1 = 22\,{\rm km\,s^{-1}}$ and $\sigma_2 = 44\,{\rm km\,s^{-1}}$. Thus the broad component seen in the integrated profile is consistent with the one we detect at all positions along our slit, which provides a further consistency check for the reality of the broad component.

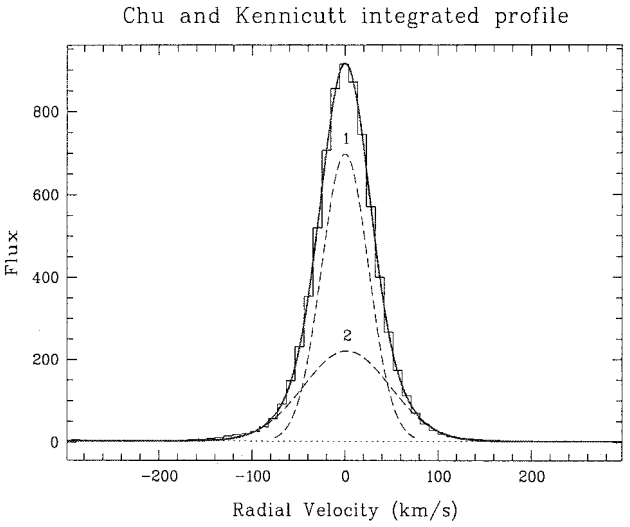

Figure 4. Integrated Hα profile from Chu & Kennicutt (1994). The profile is very well fitted by two Gaussians of widths 26 and $45.5\,{\rm km\,s^{-1}}$.

5 DISCUSSION

The high spectral and spatial resolution observations of the Hα line profile at a large number of lines of sight through the 30 Dor nebula indicate that the integrated line profile is due to the superposition of a discrete number of clouds, shells and filaments which are resolved on scales of 0.1 pc. Even very close to the nebular core, our observations show no evidence for unresolved components of supersonic velocity widths, beyond the faint, very broad component described below. While this is consistent with previous observations of this and other nebulae, it is in sharp contrast with what is seen in NGC 604, the largest H II region in M33, where the line profiles are supersonic over the whole nebula. Since the kinematical state of the nebular gas may in principle reflect the entire star formation history of the regions, the marked difference in the kinematics of the two nebulae may be due to difference evolutionary histories, as suggested by Muñoz-Tuñón et al. (1996), to differences in total mass, or to beam-dilution effects. The last, however, are unlikely because, although M33 was observed with a resolution of several parsecs, compared to 0.1 pc for 30 Dor, the radial velocity dispersion of the individual components of the line profiles near the core of NGC 604 is only a few $\rm km\,s^{-1}$, so enlarging the beam there would not broaden the components significantly. Moreover, NGC 588 presents narrower lines. It seems clear, therefore, that NGC 604 is not just 30 Dor at a larger distance. Thus it seems well established that, while winds and gravity are the dominant sources of gas kinetic energy in NGC 604, gravity appears to play no role in 30 Dor and NGC 588. In order to clarify the situation, it is crucial to map the complete 30 Dor nebula at high spatial resolution using an imaging Fabry–Pérot interferometer.

An unexpected result from our observations is the presence of an extremely broad component ($\sigma \sim 45\,{\rm km\,s^{-1}}$) which appears in all lines of sight. This component cannot be due to hot gas, since the

implied temperature would be too high for the gas to emit significantly at Hα. The presence of very broad wings in the integrated profile was already remarked by C&K who ascribed it to numerous faint shells and filaments in the outer regions of the nebula. However, the component is visible at all lines of sight throughout the nebula, and not only in the integrated profile. This suggests that the nebula is pervaded by tenuous highly turbulent diffuse component. This diffuse ionized component may originate in Champagne flows arising from the photo-erosion of denser clumps of gas, both ionized and neutral (Yorke, Tenorio-Tagle & Bodenheimer 1985). Whatever its origin, the broad component seems to be related to 30 Doradus rather than to the global LMC ISM, since it appears at the radial velocity of the nebula.

Giant H II regions and their high-luminosity sisters, the H II galaxies, are very interesting cosmological probes. Owing to the correlation between emission-line luminosity and widths, the distances to these objects can be determined out to redshifts $z > 1$with the present generation of telescopes and instrumentation. The future generation of telescopes, with its powerful suite of infrared instruments, is likely to extend this range to even larger redshifts. It is therefore of critical importance to understand the physics underlying this correlation (which, in fact, parallels the fundamental plane for spheroidal galaxies). GH IIRs have an important advantage in that detailed investigations of the kinematics of gas and stars are possible.

We have seen that the integrated emission-line-profile widths can result from very different physical processes, all of which are likely to act simultaneously with different weights according to the evolutionary status or history of the regions. On the other hand, the scaling relations between line-width, radius, and luminosity imply that the ultimate source of gas kinetic energy is the total mass within the H II regions. Taken together, these two observations imply that the initial mass functions and the evolutionary paths of GH IIRs must present very interesting regularities that may provide valuable clues to understanding galaxy and chemical evolution in the Universe.

In order to progress along this path, a number of new venues open with modern instrumentation. Deep near-infrared images covering a wide field can provide important constraints on the presence of low-mass stars in nearby GH IIRs, and thus on their role in stirring the gas. High-dispersion spectroscopy of the more massive stars will provide direct measures of the dynamical masses, which should be compared with the values derived from the gas kinematics. Accurate ground-based photometry, combined with *HST* data, will provide direct determinations of the IMF and thus of the total stellar mass. Spectral atlases are needed to establish the masses of the hotter stars, and to study the reddening laws. Many of these studies are now in progress, and results should be ripe by the time high-accuracy data on objects at cosmological distances start to be produced by the next generation of ground-based and space telescopes.

REFERENCES

Busarello G., Capaccioli M., Capozziello S., Longo G., Puddu E., 1997, A&A, 320, 415
Chu Y.-H., Kennicutt R., 1994, ApJ, 425, 720 (C&K)
Dyson J.E., 1979, A&A, 73, 132
Gallagher J.S., Hunter D.A., 1983, ApJ, 274, 141
Hippelein H.H., 1986, A&A, 160, 374
Hunter D.A. et al., 1995, ApJ, 444, 758
Meaburn J., 1981, MNRAS, 196, 19P
Meaburn J., 1984, MNRAS, 211, 521
Medina-Tanco G., Sabalisck N, Jatenco-Pereira V., Opher R., 1997, ApJ, 487, 163
Melnick J., 1977, ApJ, 213, 15
Melnick J., Moles M., Terlevich R., Garcia-Pelayo J.M., 1987, MNRAS, 226, 849
Melnick J., Terlevich R., Moles M., 1988, MNRAS, 235, 313
Muñoz-Tuñón C., 1994, in Tenorio-Tagle G., ed., Violent Star Formation: From 30 Doradus to QSOs. Cambridge Univ. Press, Cambridge, p. 25
Muñoz-Tuñón C., Tenorio-Tagle G., Castañeda H.O., Terlevich R., 1996, AJ, 112, 1636
Poglitsch A. et al., 1995, ApJ, 454, 293
Rosa M., Solf J., 1984, A&A, 130, 29
Roy J.R., Arsenault R., Joncas G., 1986, ApJ, 300, 624
Smith M.G., Weedman D., 1972, ApJ, 172, 307
Tenorio-Tagle G., Muñoz-Tuñón C., Cox D., 1993, ApJ, 418, 767
Tenorio-Tagle G., Muñoz-Tuñón C., Cid-Fernandez R., 1996, ApJ, 456, 264
Tenorio-Tagle G., Muñoz-Tuñón C., Pérez E., Melnick J., 1997, ApJ, 490, L179
Terlevich R., Melnick J., 1981, MNRAS, 195, 839
Yang H, Chu Y.-H., Skillman E.D., Terlevich R., 1996, AJ, 112, 146
Yorke H.W., Tenorio-Tagle G., Bodenheimer P., 1985, A&A, 138, 325

This paper has been typeset from a TEX/LATEX file prepared by the author.